

A NOVEL APPROACH FOR THE STRUCTURAL INTEGRITY ASSESSMENT OF CANDU REACTOR PRESSURE TUBES

Alexandra JINGA¹, Mărioara ABRUDEANU², Vasile RADU³, Livia STOICA⁴,
Alexandru NITU⁵, Denisa TOMA⁶

The CANDU reactor pressure tubes are vulnerable to a detrimental event known as Delayed Hydride Cracking under normal operating conditions (DHC). The current work offers a novel method for assessing the structural integrity of the DHC initiation at the pressure tube's blunt defects. Based on the results of the experiments, the technique uses Failure Assessment Diagrams.

Keywords: CANDU reactor, pressure tubes, hydride cracking, failure assessment diagram

1. Introduction

Two CANDU-type nuclear power units are now operating in Romania at the Cernavoda site. Natural uranium is used in the CANDU Unit reactor, while heavy water is used as the coolant and moderator. The fuel bundles are housed in pressure tubes composed of Zr-2.5%Nb that also use heavy water at high pressure (10 MPa) and a temperature range of 260°C (inlet) to 310°C as a coolant (outlet). The so-called "annulus gas" fills the area between the pressure tubes and the calandria tubes inside the fuel channels, and four fixed garter springs keep these tubes apart [1].

The pressure tubes have an internal diameter of 103 mm, a wall thickness of 4 mm, and are constructed from a cold-worked Zr-2.5%Nb alloy. The stainless-steel end fittings are formed by rolling them. When the pressure tubes are used normally, they are susceptible to a slow corrosion process that causes the tube body to gradually accumulate deuterium (Fig. 1(a)). The crack initiation and propagation process identified as Delayed Hydride Cracking (DHC) occurs in pressure tubes when the original hydrogen plus absorbed deuterium concentration in the tube exceeds the terminal solid solubility. As a result, the structural integrity assessment should be completed based on the findings of the in-service inspection. The

¹ Eng., Institute for Nuclear Research, Pitești, Romania, e-mail: alexandra.jinga@nuclear.ro

² Emeritus Prof., University of Pitești, Romania, e-mail: abrudeanu@gmail.com

³ PhD Phys., Institute for Nuclear Research, Pitești, Romania, e-mail: vasile.radu@nuclear.ro

⁴ PhD Eng., Institute for Nuclear Research, Pitești, Romania, e-mail: livia.stoica@nuclear.ro

⁵ PhD Eng., Institute for Nuclear Research, Pitești, Romania, e-mail: alexandru.nitu@nuclear.ro

⁶ Eng., Institute for Nuclear Research, Pitești, Romania, e-mail: denisa.toma@nuclear.ro

concentration of deuterium (equivalent hydrogen) at the ends of the pressure tube surpasses the solubility limit (30 ppm) in the solid state in the second part of the planned lifetime at temperatures in the range of 260°C to 310°C (Fig. 1(b)).

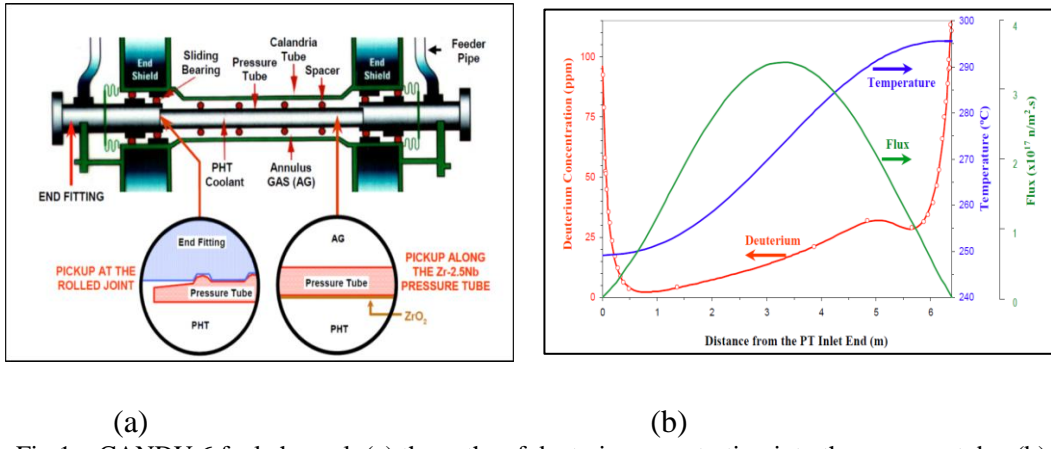


Fig.1 – CANDU 6 fuel channel: (a) the paths of deuterium penetration into the pressure tube, (b) deuterium concentration, temperature and neutron flux along the CANDU 6 pressure tube [1]

Delayed hydride cracking is a multi-step, diffusion-controlled crack propagation mechanism. Hydrogen (or deuterium) atoms diffuse to a spot tensile stress area of the tube surface. These spots are the crack or notch tips loaded by tensile hoop stress, as a result of the internal pressure of the coolant. The hydride (δ -hydride, $\text{ZrH}_{1.6}$) precipitation, which is the brittle phase of the zirconium, happens if the hydrogen concentration at these sites reaches thermal solid solubility. The hydride normals are positioned parallel to the pressure tubes' hoop direction, which corresponds to the direction of applied tensile stress. Fractures of "radially reorientated" hydrides will happen when the crack/notch tip hydride reaches a certain size, and the stated process will repeat itself [2, 3].

Fretting of bearing pads, crevice corrosion at the locations of the fuel bundle bearing pads, fretting of debris, and fuel bundle scratching during refuelling are the most frequent flaws of the pressure tubes in CANDU reactors that have been discovered through periodic examination. In this context, debris fretting is a recognized in-service damage mechanism that results in pressure tube flaws deeper than the acceptability standard (0.15mm) of CSA Standard N285.4 [4]. As shown in Fig. 2, the bulk of debris fretting damage in CANDU pressure tubes has been confined, shallow, blunt notches with low-strain concentration.

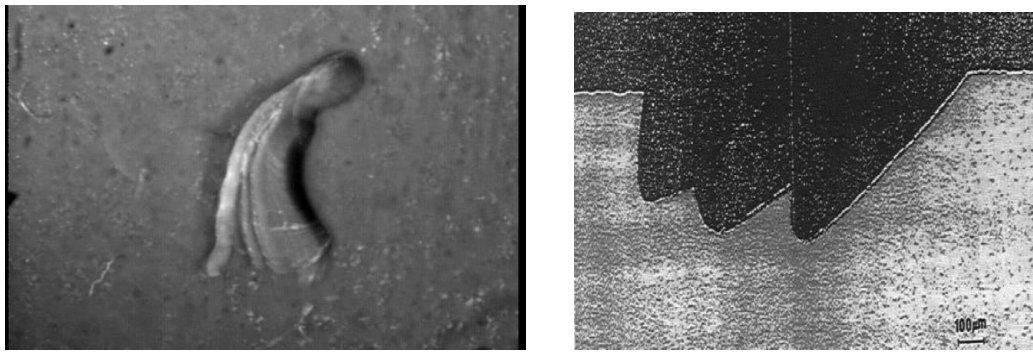


Fig. 2 – Examples of debris fret on the inner pressure tube surface: (a) (replica) [5], (b) transverse section [1]

According to British Procedure R6 [6], using a Failure Assessment Diagram, two criteria—fracture and plastic collapse—are used to assess the structural integrity in relation to the limiting conditions (FAD). The failure assessment diagram must have points drawn on it, with the locations of each assessment point depending on the applied load, the magnitude of the flaw, the characteristics of the material, etc.

The evaluation in the current study accounts the experimental findings and is based on the Failure Assessment Diagrams in the form created for Zr-2.5%Nb pressure tubes by D.A. Scarth and T.E. Smith [7, 8]. This FAD is designed to evaluate the likelihood of DHC starting at blunt flaw under normal operating conditions.

The paper also includes the experimental findings of experiments that were done to reorient the hydrides at the blunt flaw-tip zone. On the basis of metallographic images, depth zones containing reoriented hydrides (ZRH) were measured. A re-evaluation of a blunt flaw with its reorientation zone as an "effective blunt flaw" is presented after comparing the depth values with those found from the finite element stress assessments at the notch-tip. The genuine blunt flaw depth and the ZRH depth are added to determine the "effective blunt flaw" depth. For the Zr-2.5%Nb pressure tube, the experimental findings and the "effective blunt flaw" assumption are used in the Failure Assessment Diagrams format, and the impact on the Failure Assessment Curve shapes is discussed.

2. Method of analysis

2.1 Failure Assessment Diagrams for blunt flaws in CANDU pressure tubes

The CANDU pressure tube (Zr-2.5%Nb alloy) is exposed to a DHC phenomenon when the hydrogen/deuterium atoms migrate to a service-induced law under a certain stress gradient and temperature field. A brittle hydrided zone will emerge at the flaw root after the TSS limit is reached, followed by the precipitation of hydride platelets on properly oriented crystallographic planes in the material matrix. The hydride ratcheting conditions are reached when the hydrogen concentration is high enough to prevent the hydrides from the flaw-surroundings tip from dissolving at the peak temperature in a heat-up and cool-down thermal cycle. The hydrided region will enlarge with each temperature cycle as a result, creating a brittle zone around the blunt flow tip. The structure of the hydrided zone differs slightly from that of the surrounding zirconium alloy matrix in a few key ways.

The process-zone concept can be used to model DHC initiation since the hydrided region is discrete in character [8]. The strip yield zone is the term given by the process zone methodology to the form of representation that describes relaxation brought on by plasticity at a stress concentration [4]. It is possible to think of a hydrided zone that escapes at a defect root and the nearby region that is fracturing as one unit (Fig. 3).

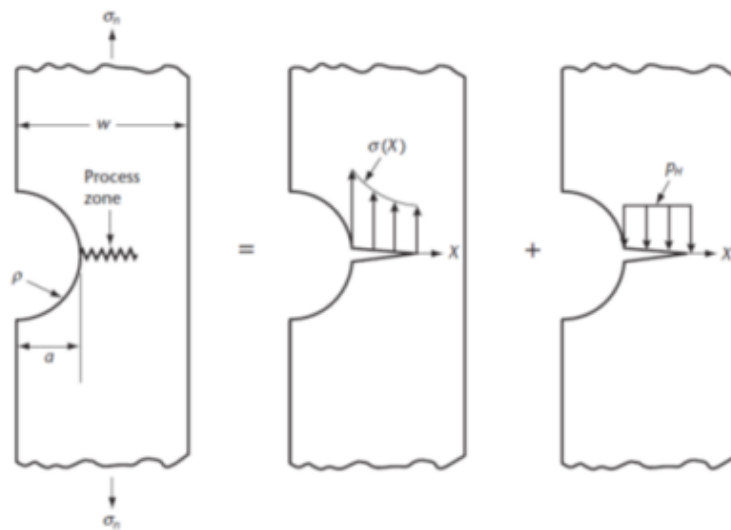


Fig. 3 – Blunt flaw geometry and characteristics in process-zone approach [4]

From the closed form mode three process zone, the Failure Assessment Diagrams for DHC initiation from blunt flaws were created. In a semi-infinite

material, Scarth described [7, 8] the anti-plane strain, the process-zone simulation of DHC initiation at the two-dimensional blunt surface flaw.

The Mode III solutions are simple and can provide insight into how various material and geometrical characteristics interact for DHC prediction using FADs, which is why this model was utilized to build the Failure Assessment Diagrams for DHC initiation [7, 8].

The Failure Assessment Diagrams for DHC initiation were developed in terms of K_r and L_r , which are defined as:

$$K_r = \frac{\sigma_n \sqrt{\pi a}}{K_{IC}} \quad (1)$$

and

$$L_r = \frac{\sigma_n}{p_c} \quad (2)$$

Where:

σ_n - applied nominal stress;

a - notch depth;

K_{IH} - threshold stress intensity factor for delayed hydride cracking initiation at a planar surface;

p_c - threshold stress for delayed hydride cracking initiation at a planar surface.

In a first attempt [7], the failure assessment curve for DHC initiation at threshold conditions is given by:

$$K_r = \frac{\pi \cdot L_r}{\left\{ 8 \cdot \ln \left[\sec \left(\frac{\pi}{2} \left(1 + \sqrt{\frac{\rho}{a}} \right) \left(L_r - \frac{1}{1 + \sqrt{\frac{\rho}{a}}} \right) \right) \right] \right\}^{1/2}} \quad (3)$$

Here ρ is the root radius at the flaw tip.

In a special case when the root radius $\rho = 0$, then $\frac{\rho}{a} = 0$, which means the semielliptical flaw merges into a crack, then Equation (3) simplified to the relation [6]:

$$K_r = \frac{\pi \cdot L_r}{\left\{ 8 \cdot \ln \left[\sec \left(\frac{\pi}{2} L_r \right) \right] \right\}^{1/2}} \quad (4)$$

Another failure assessment diagram in the unique format, $K_{rs} - L_{rs}$, from Mode III simulation of Mode I loading of a semielliptical flaw in the semi-infinite material was produced to diminish the geometry relying in Equation (3) [7, 8]:

$$K_{rs} = \frac{\pi \cdot L_{rs} \cdot \left(1 + \sqrt{\frac{\rho}{a}}\right)}{\left\{8 \cdot \ln \left[\sec \left(\frac{\pi}{2} \left(1 + \sqrt{\frac{\rho}{a}}\right) \left(L_{rs} - \frac{1}{1 + \sqrt{\frac{\rho}{a}}} \right) \right) \right] \right\}^{1/2} + \pi \cdot \sqrt{\frac{\rho}{a}}} \quad (5)$$

The coordinates of the assessment point for a certain configuration of flaw and loading, are given by:

$$K_{0rs} = \frac{\sigma_p}{p_c + \frac{K_{IH}}{\sqrt{\pi\rho}}} \quad (6)$$

And

$$L_{0rs} = \frac{\sigma_n}{p_c} \quad (7)$$

The failure assessment point (K_{0rs}, L_{0rs}) will lie on a line from the origin [7]:

$$K_{0rs} = \left[\frac{1 + \sqrt{\frac{a}{\rho}}}{1 + \frac{K_{IH}}{p_c \sqrt{\pi\rho}}} \right] \cdot L_{0rs} \quad (8)$$

For the certain geometric values of the flaw, a, ρ , and considering $p_c = 450 \text{ MPa}$, $K_{IH} = 4.5 \text{ MPa} \cdot \sqrt{m}$, that is the case of Zr-2.5%Nb alloy, then by varying applied loading, the onset of DHC initiation is predicted at the point where line (8) intersects the failure assessment curve (Equation (5)).

2.2 Experimental procedure for hydride precipitation and reorientation at the blunt flaw in CANDU pressure tube

While zirconium hydrides are present in Zr-2.5%Nb pressure tubes at room temperature, they only precipitate at 250°C to 300°C temperatures in CANDU fuel channels, when the hydrogen equivalent concentration, abbreviated H_{eq} , is higher than the terminal solid solubility. The hydrogen equivalent concentration, H_{eq} , is the result of adding the hydrogen concentration found in a brand-new tube with the half-concentration of deuterium obtained during the service. Depending on the tube temperature, the terminal solid solubility at operating pressure ranges from 35 to 75 ppm. The hydrogen content of Zr-2.5%Nb pressure tubes has been lowered to less than 5 ppm thanks to recent advancements in manufacturing processes. The thickening of the oxide layer occurs as a result of the heavy water passing through the pressure tubes during CANDU reactor operation. It should be noted that around 5% of the deuterium produced by corrosion is absorbed by the Zr-2.5%Nb pressure tubes.

For the present study, the experimental works used a specimen having a “V-type” notch, on the inside surface, Fig. 4. The range of flaw depth was $a = 0.2 \div 0.3 \text{ mm}$, and the root radius $\rho = 0.07 \div 0.1 \text{ mm}$.

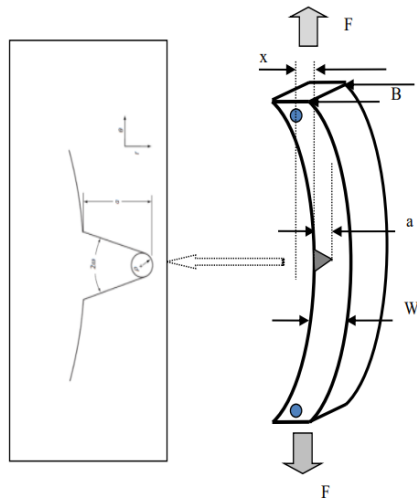


Fig. 4 – C-shape specimen, Zr-2.5%Nb, used in the experimental work

The electrolytic method has been used to obtain the hydride specimens at various levels of hydrogen concentration. The following are the steps in the electrolytic method: A hydride layer is sited on the Zr-2.5%Nb specimen surface, using $0.1\text{ H}_2\text{SO}_4$ electrolyte at temperature of 90°C , and 100 mA/cm^2 current density; A heat treatment at 400°C is applied to promote the diffusion of hydrogen in the specimen body. Fig. 5(a) in the transversal-radial section shows zirconium hydrides precipitating, and the hydrogen concentration is in the range of 35-75 ppm. The Zr-2.5%Nb pressure tubes are extremely textured, and the majority of the hydride platelets are oriented in the circumferential direction.

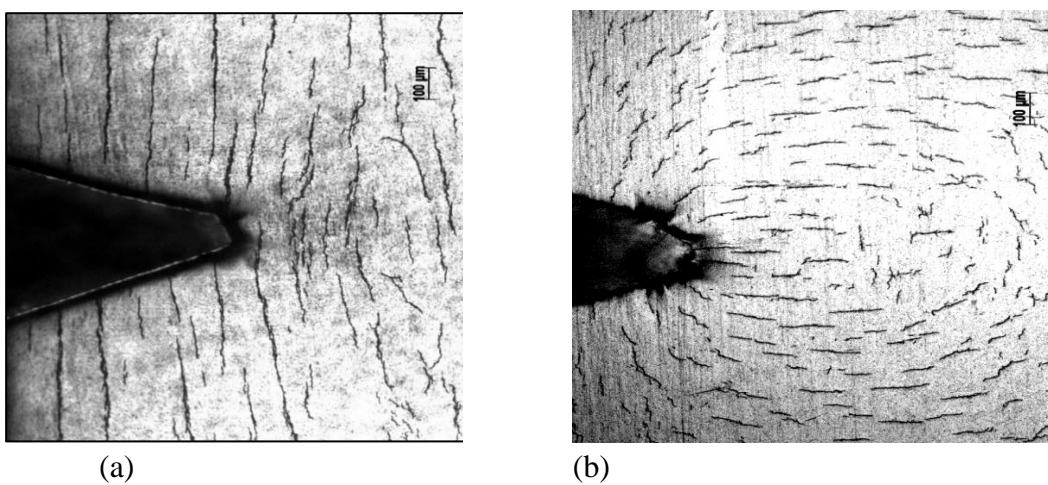


Fig. 5 – Metallographically aspects of hydride orientation: (a) original precipitation of the zirconium hydrides in Zr-2.5%Nb, (b) hydride reorientation at notch tip, (65 ppm of hydrogen)

The stress should be around 240 MPa at the flaw tip at a temperature of 270°C to initiate the reorientation hydrides phenomenon in Zr-2.5%Nb specimens from the circumferential direction in the radial direction of the pressure tube wall. Fig. 5(b) depicts a portion of hydride reorientation at the defect tip.

To perform the "hydride platelets reorientation" the following procedure was used:

- Increase the tensile loading on the specimen up to a defined nominal stress;
- Maintaining the load at a constant level;
- Applying a thermal treatment, with thermal cycle sequences as in Fig. 6.

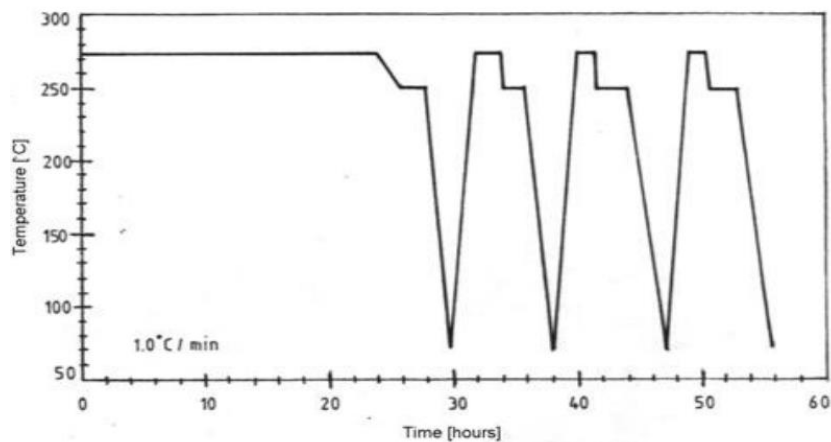


Fig. 6 – Thermal cycles for hydride reorientation

Examining the metallographic analyses in Fig. 5(b), it can be seen that the hydride platelets are reoriented in an approximately circular zone at the flaw tip. These zones are referred to as "zone with reoriented hydrides" (ZRH), and the degree of mechanical stress determines how big they are.

3. Results analysis and new approach for the structural integrity analysis by FAD

Using the same stress loading conditions as the experimental work, a finite element analysis was performed to estimate the magnitude of ZRH (Fig. 7 (a)).

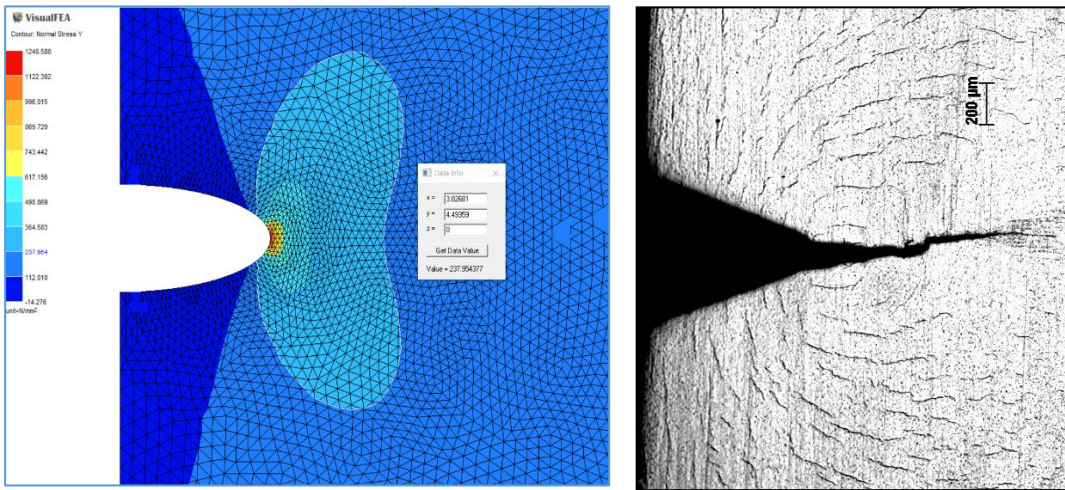


Fig. 7 – (a) Finite element analysis of flaw tip zone, (b) cracking of ZRH through hydrides

Fig. 7(a) shows the size and form of the zone surrounding the flaw tip, which has a stress of at least 240 MPa and is of a similar magnitude to the ZRH found in metallographic analyses.

In comparison to the zirconium ductile matrix, the hydride **ZrH_{1.6}** is extremely brittle, and the critical stress intensity factor has a value in the range $K_{Ic}=1\text{--}3$ MPa. Fig. 7(b) illustrates what happens when the number of heat cycles is increased under a constant tensile load: fracture start and growth through the hydride reorientation zone. The stress intensity factor for a blunt flaw in this last image is $K_I = 12.2 \text{ MPa}\sqrt{m}$ (estimated for a crack with the same two-dimensional dimensions), and N=17 thermal cycles are present. Zirconium hydrides that are broken off perpendicular to the surface tip of the notch cause the crack to spread through the DHC mechanism. The DHC crack is expanding in a radial direction to a depth of approximately 400 μm . The brittle filaments of the reoriented hydrides were fractured to achieve crack penetration, and given the size of the DHC crack in Fig. 8(b) and the fact that it developed quickly during the most recent thermal cycles, the hypothesis of a limited number of brittle fracture sequences is put forth. A brittle crack generally progresses along a brittle line of connected hydride filaments in the area of localized hydride reorientation, with its front oriented perpendicular to the direction of mechanical force. As anticipated, at this level of K_I factor value, fracture propagation ceases only when the crack tip touches the ductile matrix of the Zr-2.5%Nb alloy. Based on these factors, we may construct an "effective blunt flaw" idea or even view the ZRH entity in front of the notch tip as "an extension" of the true flaw. Since real notch depth and ZRH depth are added together, we consider the depth of the effective blunt flaw to be equal.

Then, using the Failure Assessment Diagram (Equation (5)) and the assessment point (Equation (8)), we examine how this concept applies to the structural integrity assessment of the CANDU pressure tube. The following blunt flaw characteristics are selected: depth of real flaw; $a = 0.3 \text{ mm}$; root radius of the flaw; $\rho = 0.05 \text{ mm}$; depth of ZRH; $a_{ZRH} = 0.2 \text{ mm}$; depth of the effective blunt flaw; $a_{eff} = 0.3 + 0.2 = 0.5 \text{ mm}$. Evaluation with the Failure Assessment Diagram of a blunt flaw with these characteristics by considering the “effective blunt flaw” concept is displayed in Fig. 8.

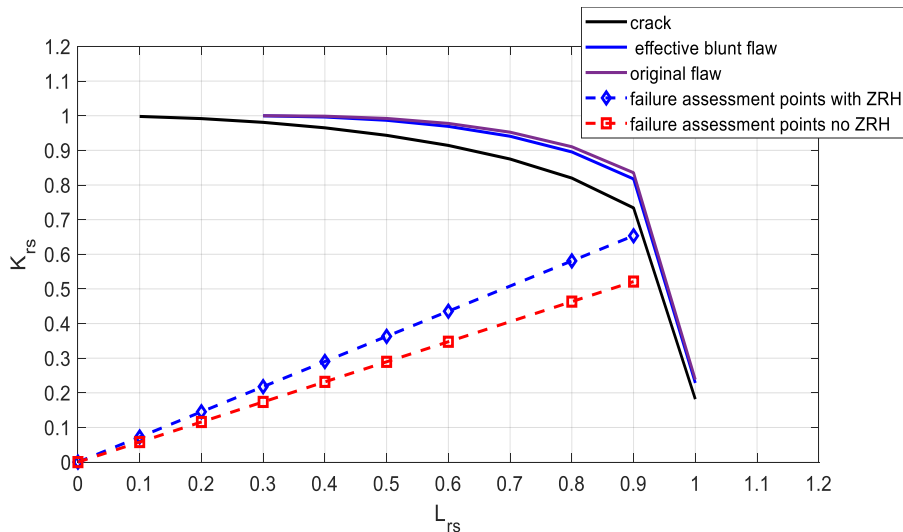


Fig. 8 – Evaluation with the Failure Assessment Diagram of a notch by considering the “effective blunt flaw” concept

The following observations may be seen by analyzing the FAD graphics:

- By using the “effective blunt flaw” concept the FAD evaluation curve is a bit closer to the FAD representation for a crack;
- FAD evaluation curve with the “effective blunt flaw” concept becomes a little more conservative than the actual flaw when the structural integrity assessment is done;
- The assessment points line, given by Equation (8), by considering the “effective blunt flaw” concept, has a higher slope than for the real flaw; this increases the probability of DHC crack initiation and growth, at the point where this line intersects the failure assessment curve.

4. Conclusions

The cold-worked Zr-2.5% Nb alloy used to made the CANDU pressure tubes is susceptible to slow corrosion under normal operating settings, which causes

deuterium to gradually accumulate in the tube body. Pressure tubes are likely to be exposed to a crack initiation and propagation practice called as Delayed Hydride Cracking (DHC) when the initial hydrogen plus absorbed deuterium concentration in the tube exceeds the terminal solid solubility (TSS). As a result, the structural integrity assessment, based on the results of the in-service inspection, should be carried out.

The current study focuses on the assessments of structural integrity of the DHC initiation at the pressure tube faults in a CANDU reactor. The failure assessment diagrams (FADs), an integrated graphical representation for the fracture failure and plastic collapse evaluation in case of blunt flaws in the pressure tubes, were used to describe the approach in the first chapter.

A "zone with reoriented hydrides" (ZRH) near the flaw tip, as well as crack initiation and growth inside these zones, were demonstrated in experimental tests on Zr-2.5%Nb specimens cut from CANDU pressure tubes. The ZRH entity in front of the notch tip was described as an "effective blunt flaw" notion and is thought to be "an extension" of the true flaw. According to this theory, the genuine notch depth plus the ZRH depth together make up the depth of the effective blunt defect.

The novel approach by "effective blunt flaw" idea has been examined when evaluating a blunt flaw using the Failure Assessment Diagram. It was determined that the FAD assessment curve is a little bit closer to the FAD representation for a crack when employing the "effective blunt defect" concept. Additionally, when the structural integrity assessment is completed, the FAD evaluation curve with the "effective blunt flaw" concept becomes a little bit more conservative than the actual flaw. By taking into account the "effective blunt flaw" idea, the assessment points line has a steeper slope than for the actual flaw. The failure evaluation curve is where this line connects, and this fact raises the likelihood of DHC crack development and growth there.

Based on the findings of in-service inspections, the study results are currently being applied to the structural integrity assessment of CANDU pressure tubes from Cernavoda NPP.

R E F E R E N C E S

- [1]. IAEA-TECDOC-1037, Assessment and management of ageing of major nuclear power components important to safety: CANDU pressure tubes, IAEA, 1998.
- [2]. Manfred P. Puls, The Effect of Hydrogen and Hydrides on the Integrity of Zirconium Alloy Components - Delayed Hydride Cracking, Copyright © Springer-Verlag London, 2012.
- [3]. Manfred P. Puls, The Effect of Hydrogen and Hydrides on the Integrity of Zirconium Alloy Components - Hydride Reorientation, Copyright © Advanced Nuclear Technology International Europe AB, ANT International, 2018.

- [4]. CAN/CSA Standard N285.4-05: Periodic inspection of CANDU nuclear power plant components, 2005.
- [5]. Michael Trelinski, Proceeding IV Conferencia Panamericana de END Buenos Aires, (2007).
- [6]. *** R6 revision 4, Assessment of the integrity of structures containing defects, Copyright © 2006 Published in the United Kingdom by British Energy Generation Ltd., 2006.
- [7]. Scarth, D.A., Smith, T.E., International Journal of Pressure Vessels and Piping, Volume **79**, Issue 3, 233-243, (2002).
- [8]. Douglas A. Scarth, Ted Smith, Proceedings Paper of Pressure Vessels and Piping Conference, PVP2003, 103-116 (2014)